Progress In Electromagnetics Research M, Vol. 94, 189–199, 2020

Printed GNSS and Bluetooth Antennas Embedded on Flexible Low Loss Substrates for Wearable Applications

Gbotemi Omodara[1], Sami Myllymäki[1, *], Heli Jantunen[1], Jari Juuti[1], Sami Ihme[2], Marika Kurkinen[2], Ville Majava[3], Marko Tuhkala[3] and Juhani Kemppainen[3]

Abstract—This paper presents Global Navigation Satellite System (GNSS) F-type and Bluetooth (BT) L-shaped antennas printed on flexible low loss substrate materials for smartwatch applications. The proposed printed antennas were designed along with the wristband of a smartwatch device with the main purpose of improving their electrical performance by using a new low loss polymer material and locating the antenna on the wrist strap. The antenna performances were simulated using CST Microwave Studio, and the prototypes were measured in a Satimo StarLab anechoic chamber. Silver printing and injection molding technologies were successfully utilized for fabricating new SEBS materials (styrene-ethylene-butylene-styrene) in wearable devices. The SEBS materials improved the radiation efficiency of the antennas by 1.6 dB for the GNSS and 2.2 dB for the BT over the previously used TPU (thermoplastic polyurethane) materials. The overmolded printed and hybrid integrated discrete antennas produced added-value for electronics fabrication thanks to its flexible and seamless integration technique. In addition, it is a low-cost mass manufacturing method. The research opens new perspectives for product definitions with a flexible, low loss material that enables better antenna performance.

1. INTRODUCTION

The research in the field of flexible and wearable electronic systems has experienced rapid development in recent years due to changes in people's lives resulting from a higher standard of living, sports and fitness trends. The development has been driven by their great promises for wellness monitoring, as well as wireless communication in various application areas such as military, public safety, and enterprise applications. Generally, the wearable electronic systems used in most wearable devices are composed of antennas, smart sensors, smart wearable materials, a user-friendly interface, software, actuators, a processor, operating systems, as well as wireless communication links and modules for data extraction, processing, and decision-making purposes [1]. It is significant that wearable devices are perhaps the smallest devices required to communicate effectively at long ranges within ISM (Industrial, Scientific and Medical), mobile, and GNSS communication bands.

Wearable antennas are one of the key RF (Radio Frequency) components that enable wireless communication and data sharing between wearable devices and portable devices such as smartwatches, smart garments, smart jewelery, fitness trackers, laptops, and mobile phones. With the integration of 2.45 GHz antennas, most smartwatches can wirelessly receive, transmit, and share real-time data such as messages and voice calls over short distances via Bluetooth systems. Likewise, GNSS antennas within smartwatches can be used for location identification and tracking of sports activities by collecting, analysing, and providing reliable data for athletes during training.

Received 23 April 2020, Accepted 9 July 2020, Scheduled 27 July 2020
* Corresponding author: Sami Myllymäki (sami.myllymaki@oulu.fi).
[1] Microelectronics Research Unit, University of Oulu, Finland. [2] VTT Technical Research Centre of Finland Ltd, Finland. [3] Polar Electro Oy, Finland.

The design of antennas desirable for wearable devices has many challenges. Perhaps the most critical one is the size of the antenna implementation in the device. Another challenge is the adverse consequence of the electromagnetic interaction between the antenna and human biological tissue. The effect can lead to detuning of the resonant frequency and alterations of antenna radiation pattern and efficiency. Since wearable antennas are to be worn on the human body, it is important for the antenna to have reliable performance such as high efficiency and suitable radiation characteristics. At the same time, the antenna should be small in size, light weight, flexible, in low profile, and simple structure for easy fabrication [2, 3].

Copper and silver are commonly used as materials for the realization of antenna conductors such as the ones presented in the wearable 915 MHz band antenna for wristwatch application [4]. Moreover, a wearable antenna located on a metal watch strap is proposed in [5] in which the width of the strap had only a small impact on the radiation patterns, but the variations of the feeding location clearly influenced the matching performance. The antenna had a bandwidth of 78% at the 2.46 GHz ISM band [5]. The wrist-wearable π-shaped antenna operating at 1575 MHz was designed with a copper conductor on a RO3210 substrate. No efficiency information was provided, but the antenna had a butterfly E-field radiation pattern on a theta 90° cut [6].

Typical antenna systems in wearable devices consist of dual or multiple band antennas. Two cellular antennas, LTE low and mid-band antennas and one GNSS antenna operating at 699–862 MHz and 1710–2155 MHz are presented in [7]. The polarization performance of the GNSS antenna was 5 dB higher for the right-hand circular polarization (RHCP) than the left-hand circular polarization (LHCP).

The device had a reasonable isolation between antennas and efficiencies of −10 dB, −6 dB, and −4 dB for the LTE low band, mid-band, and GNSS band [7]. In addition, four-band antenna structures were presented providing radiation efficiencies of −6 dB at 810–960 MHz, −2 dB at 1370–1450 MHz, and −2 dB at 1710–1630 MHz for LTE/WCDMA bands and −1 dB for the ISM band in the free space environment. The antenna radiation efficiency was reduced to a half by the hand phantom [8]. With wrist wearables, the bending effect of the antenna is reasonable. The performance of a textile-patch antenna operating at a 2.4-GHz ISM band was evaluated. The substrate denim textile and conductors are made of copper and nickel-plated polyester fabrics presenting a gain of 4 dBi and 70° of the half-power beamwidth (HPBW) in a straight position and a gain of 2 dBi and an HPBW of 95° in the bent position [9]. A low profile 0.1 mm thick polyimide substrate $\varepsilon_r = 3.4$) and loss tangent ($\tan\delta = 0.002$) with a copper layer of thickness 18 µm was used for a compact planar wearable antenna, i.e., the bowtie design principle and miniaturization techniques to achieve dimensions of $0.2\lambda \times 0.13\lambda$ for the GNSS band. The antenna changes its polarization discrimination either on linear or circular polarization by varying its physical configurations. The radiation efficiency of the antenna was −0.2 dB in free space and −19 dB at a close proximity to hand (1 mm) [10]. Even at higher frequency bands, a dual-band antenna with circular polarization was designed for ISM and 5 GHz WLAN band applications. The antenna on an RT Duroid substrate with dimensions of $40 \times 28 \times 0.4\,\text{mm}^3$ was fed by a coplanar waveguide with an asymmetric ground structure having the impedance bandwidths of 39% and 49% for operating bands, and a 3 dB axial ratio bandwidth of 150 MHz at lower and 1600 MHz at higher bands [11]. Also, a flexible compact UWB MIMO/diversity antenna system was presented in wearable antennas. The antenna was a thin printed 50 µm Kapton Polyimide substrate consisting of two half-elliptical shaped radiating elements with a waveguide feed. The antenna array achieved wide impedance bandwidth, good isolation between antenna elements, and good resistance for performance deterioration due to mechanical bending [12].

A dual-band (2.45/5.8 GHz) operated, dual-polarized wearable antenna was proposed for on-body applications. The 2.45 band antenna provided 0 dB gain, and the body effect was tested with 5, 8, and 11 mm distances [13]. An ultra-wide band antenna operating in LTE bands (698–960, 1710–2170, and 2500–2700 MHz) was presented for wearable wrist worn applications in [14]. The antenna with a size of 127 mm × 25 mm × 0.13 mm was built on a flexible and very thin Kapton material. Flores-Cuadras et al. [17] obtained simulated SAR (Specific Absorption Rate) results of 3.75 W/kg at 850 MHz, 3.59 W/kg at 1900 MHz, and 3.45 W/kg at 2600 MHz with maximum EM (Electromagnetic) exposure limited to 4 W/kg ($\text{SAR}_{10\,g}$) by the FCC (Federal Communication Commission). A folded Alford loop antenna was proposed for a wireless body area network for 2.45/5.8 GHz bands [15]. The antenna provided 6/2 dBi gains for the bands, and the designed operating distance to the body was 5 mm. In addition,

a similar kind of dual band dual mode (2.5/5.8 GHz) triangular textile patch antenna was presented in [16]. The antenna was also measured at 5 mm from the body. It provided 4 dB gain in free space and 3.8 dB on the body at the 2.5 GHz frequency range.

In this paper, we designed, fabricated, and measured a dual antenna structure (GNSS/BT) for wrist band applications. The research questions are what are the benefits of using a low loss polymer substrate on the wrist band (material perspective) to the antenna and how beneficial it is to utilize wrist straps as a substrate for antenna integration (device perspective). The design is applied at a distance of less than 1 mm from the body.

2. ANTENNA DESIGN AND MATERIAL SELECTION

Two antennas were designed and fabricated on a wrist band strip, and the electronic device was located in the middle of the band. Fig. 1 shows the design geometry of the proposed GNSS and BT antennas printed (silver, Asahi LS-411A) on the wristband of a smartwatch with antennas on both sides of the wrist strap. The BT antenna was designed on the right side and the GNSS antenna on the left side of the strip. Fig. 2 presents fabricated prototypes and layout properties. The antennas were designed along the wristband primarily for demonstrating a new technology as well as to obtain higher electrical performance. The antennas were printed on a PET (polyethylene terephthalate) substrate and later injection molded into SEBS/TPU materials in such a way that the antenna was located between the PET and the molded polymer material. The antennas were connected to the device via pin connectors, and the mechanical and electrical contacts were properly connected when the device was assembled against the wrist strap.

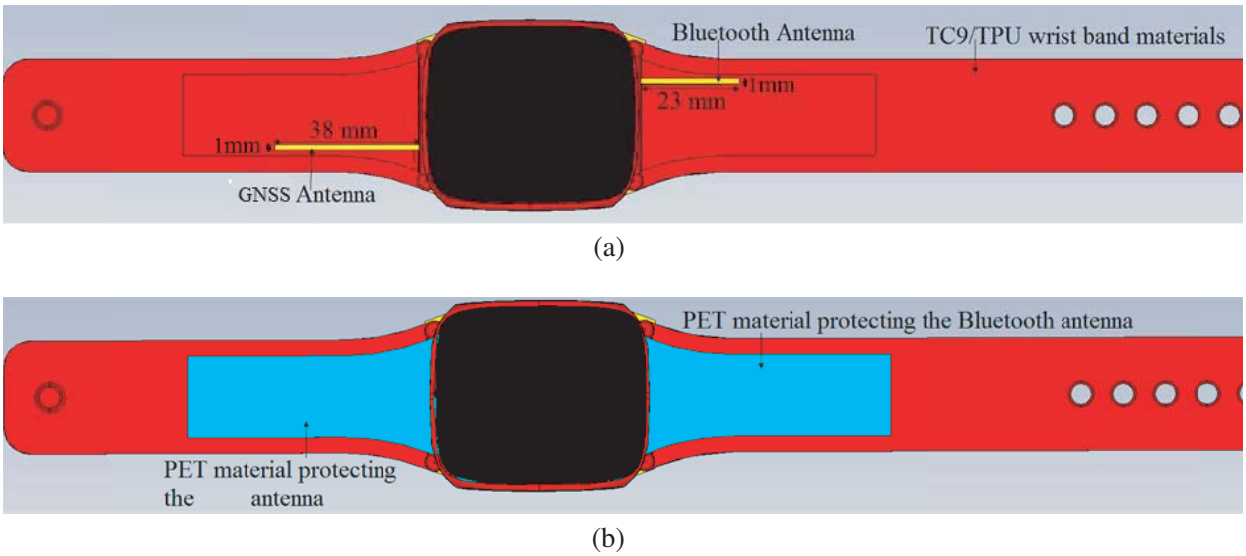

Figure 1. Proposed antenna configuration, (a) printed on a wristband in a free space model, (b) covered and protected with PET material.

The BT antenna is a straight line starting from one pin that is 1.5 mm high on top of the device's main board. The GNSS antenna has both the signal pin and ground pin located close to the feed as presented in Fig. 2. A 3 pF shunt capacitor was used for the GNSS antenna's impedance matching circuit. The total sizes of the GNSS and BT antenna radiators were 38 mm × 1 mm × 0.015 mm and 23 mm × 1 mm × 0.015 mm. Two flexible materials were used in the injection molding process; TPU (manufacturer: Lubrizol) and low loss SEBS (manufacturer: Kraiburg TPE, TC9) polymer materials with different dielectric constants and thicknesses. The materials properties are displayed in Table 1. Because the structure was injection molded the materials stuck together in the high temperature (190°C) polymer molding process. The thickness of the TPU/SEBSmaterials was 3.6 mm, and the thickness of

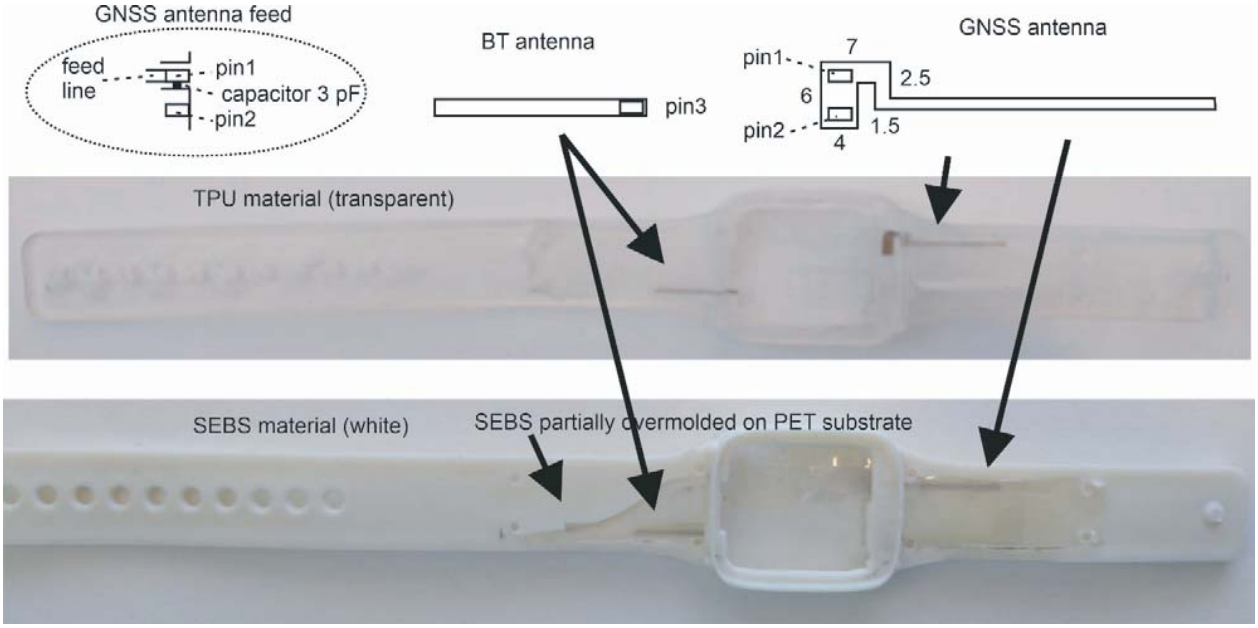

Figure 2. Proposed fabricated prototypes of TPU and SEBS materials, where GNSS and BT antennas are located between the thin PET substrate and the injection molding materials. The connection and feed structures utilized pin connectors with a 3 pF shunt capacitor. Dimensions are in millimetres.

Table 1. Material properties (2 GHz) of smartwatch wristband materials (TPU, SEBS and PET).

Materials	Thickness (mm)	Permittivity, ε	Loss Tangent, $\tan\delta$
TPU	3.6	2.9	0.05000
TC9	3.6	2.7	0.00067
PET	0.125	2.7	0.00025

the PET was 0.125 mm. The permittivity and dielectric loss tangents were 2.9/0.05 for TPU, 2.7/0.0007 for SEBS and 2.7/0.00025 for the PET materials. The dielectric properties of the set of materials were measured in a broad range with an Agilent Impedance Analyser (10 MHz–1 GHz) and Split Post Dielectric Resonator (SPDR 2.45 GHz).

Optimizing the material properties in the antenna structure is important for maximizing device performance. In the vicinity of the antenna, materials should obtain low dielectric losses. At the moment, commonly used materials such as TPU exhibit rather high loss performance. At the same time, the operation conditions such as temperatures down to -40°C should not change their mechanical form and harm the device. The materials should provide sufficient mechanical ruggedness, hardness, and comfort for the user. Naturally the materials should also meet the requirements of RoHS (Restriction of Hazardous Substances Directive) and REACH (Registration, Evaluation, Authorisation and Restriction of Chemicals). For these reasons, TPU/SEBSthermoplastic elastomer materials were selected for antenna materials, and their electrical properties at high frequencies were not widely known. Elastomer is a material that elongates at least 100% when being influenced by an external force and recovers when the external force is deforced. Rubbers are elastomers that are cross-linked with covalent bonds. Thermoplastic elastomers are elastomers whose molecules are bonded with secondary bonds and therefore can be injection moulded with heat and pressure.

The process steps for fabricating the device and antenna were:

1. Printing of antenna patterns on a PET substrate with R2R (roll-to-roll) screen printing.
2. Cut-out with ultraviolet laser.

3. Overmolding (Engel Victory 120) of the antenna prints with SEBS or TPU, PE (polyethylene) PSA (pressure sensitive adhesive) laminate was used in the case of SEBS for the adhesion.
4. Assembling of device mock-up with SMA (SubMiniature version A) female connectors for antenna measurements.

3. RESULTS AND DISCUSSIONS

The performance of the antenna was simulated using CST microwave studio, and the prototypes were measured in a Satimo Starlab anechoic chamber. Antenna performance factors such as the reflection coefficient of the input port, 2-dimensional radiation patterns, gain, and the total efficiency (in free space) of the proposed antenna were measured. In addition, corresponding 3-dimensional radiation patterns, user hand-induced effect, and antenna bending effects were simulated. SAR (specific

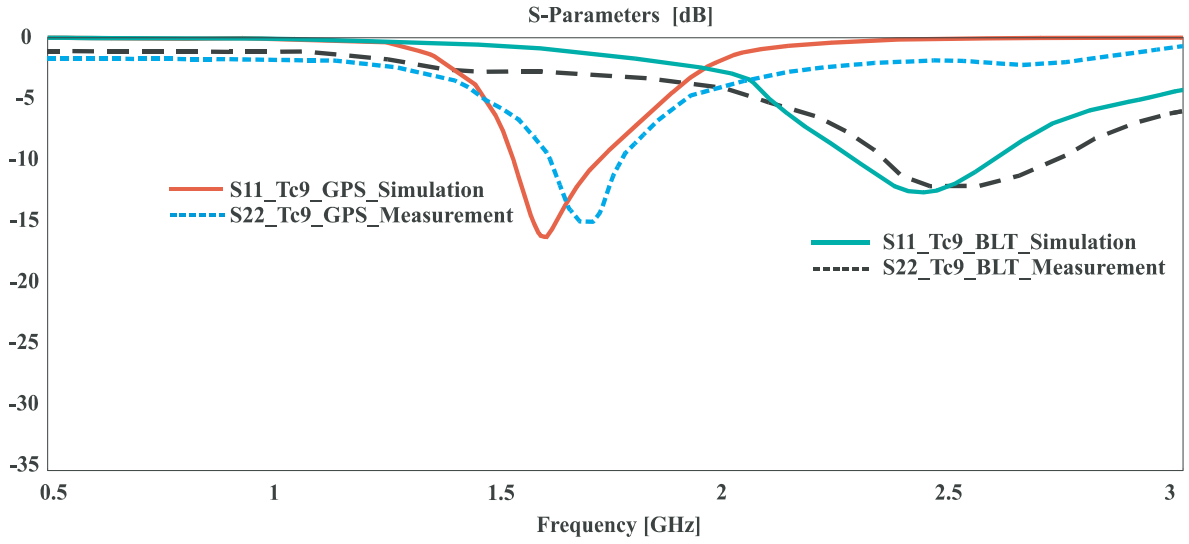

(a)

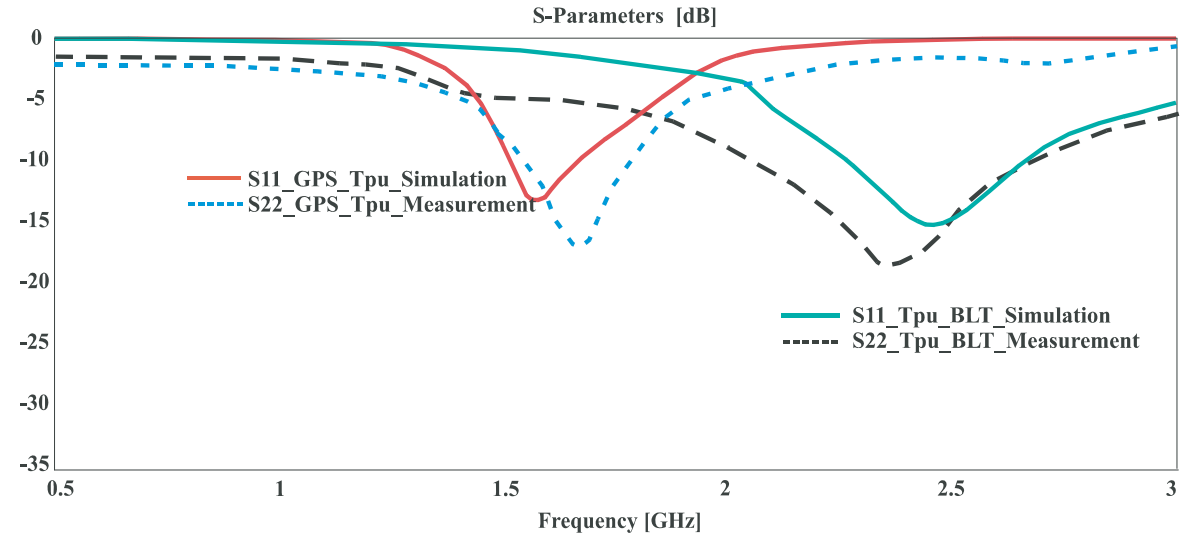

(b)

Figure 3. Simulated and measured reflection coefficients of the proposedGNSS/BT antennas with (a) SEBS (TC9) and (b) TPU, materials.

absorption rate) values were calculated with the BT antenna with the class 2 standard power of 2.5 mW. Polarization measurements for GNSS were not carried out in this study.

The measured and simulated reflection coefficients of the antenna with both the SEBS and TPU materials integration are shown in Fig. 3. The center frequency and impedance matching bandwidth of the GNSS antenna with SEBS material were 1.58 GHz/280 MHz for simulated results and 1.68 GHz/330 MHz for measured results, respectively. The center frequency and matching bandwidth of the BT antenna with SEBS material were 2.45 GHz/550 MHz for simulated results and 2.50 GHz/830 MHz for measured results. The measured center frequency values were slightly higher than the simulated ones most likely due to dimensional shrinkage of the device material. The measured bandwidth values were slightly larger than the simulated ones most likely due to the slightly lower than expected conductivity of the printed silver materials. Manual handling of prototypes caused some fluctuations in matching measurements.

The center frequency and impedance matching bandwidth of the GNSS antenna with TPU material were 1.58 GHz/250 MHz for the simulated results and 1.65 GHz/350 MHz for the measured results, respectively. The BT antenna with TPU materials had the corresponding values of 2.45 GHz/500 MHz for the simulated results and 2.50 GHz/800 MHz for the measured results. Similar trends in the relation between the simulated and measured results with TPU material can be observed with SEBS material.

The measured antenna parameters such as directivity, gain, and efficiency values of GNSS and Bluetooth antennas with the integration of the low loss materials (TC9, TPU and PET) are given in Table 2. The directivities of the GNSS and BT antennas were 2.6 dBi and 2.8 dBi. The total efficiencies for the GNSS with SEBS and TPU were measured to be −10.9 dB and −9.4 dB, respectively. The total efficiencies for the BT antenna were measured to be −4.8 dB with TPU and −2.7 dB with SEBS materials. Antenna gains were −8.2 dB/−6.6 dB for GNSS antennas and −1.9 dB/0.3 dB for BT antennas with different materials. The SEBS (TC9) flexible substrate material improves the efficiencies of both the GNSS antenna by 1.6 dB and Bluetooth antenna by 2.2 dB. Compared to [4–11], the current improvements are remarkable for replacing previous printed circuit board materials with molded polymers in which the loss levels are very competitive.

Table 2. Antenna directivity, gain and efficiency results for the proposed GNSS and Bluetooth antennas.

Measured Parameters	GNSS plus PET and TPU	GNSS plus PET and SEBS	BT plus PET and TPU	BT plus PET and SEBS
Directivity (dBi)	+2.6	+2.6	+2.8	+2.8
Gain (dB)	−8.2	−6.6	−1.9	0.3
Total Efficiency (dB)	−10.9	−9.4	−4.8	−2.7
Return Loss (dB)	18.1	15.1	19.4	14.0
Mismatch Loss (dB)	0.1	0.2	0.1	0.2
Radiation efficiency (dB)	−10.8	−9.2	−4.7	−2.5

Antenna radiation patterns were measured in a Satimo Starlab system in free space and the axis cuts are presented in Fig. 4. The electronic device was installed in the wrist band, and the cables were soldered to the connection pin of the antenna. Simulated antenna 3-dimensional directivity patterns are presented in Fig. 5. Both GNSS and BT antennas provided monopole kinds of patterns in free space, both located similarly on opposite directions of the device.

Both GNSS and BT antenna 2-dimensional gain patterns at phi0 and phi90 cuts with SEBS materials are presented in Fig. 6. The simulated results present the comparison of (1) the antenna in free space, (2) the antenna located on the hand in a straight position (i.e., not bent), and finally (3)

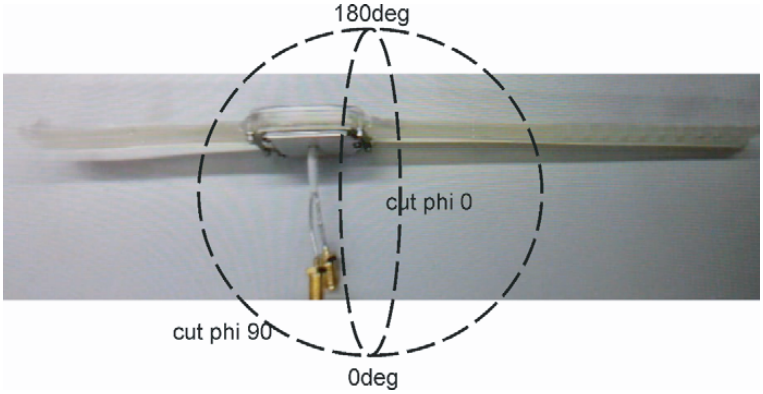

Figure 4. Picture of prototype and illustration of how the cut axes (phi0 and phi90) of the antenna pattern were arranged in free space measurements.

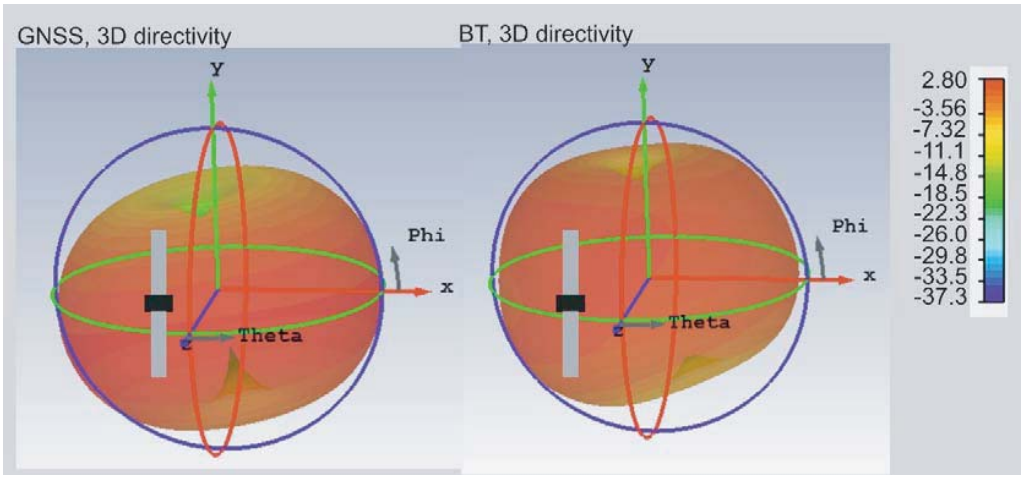

Figure 5. Simulated 3-dimensional directivity patterns of the GNSS and BT antennas in free space.

the antenna located on the hand in a bent position. In position (3) the strip of wristwatch was located tightly on the surface of the hand, resulting in an only 0.8 mm distance between the antenna and the body.

Based on the simulated results of the GNSS antenna, in close proximity to the hand the antenna performance decreased to −19 dB gain. The antenna pattern in the phi0 cut changed from omnidirectional to directive with the maximum at 0 degrees. The difference between the antenna bent to the hand and the antenna in straight positions is 3 dB. In addition, the antenna pattern in the phi90 cut changed away from the hand towards 0 degrees, but the pattern is not as symmetric as the phi0 cut due to the position of the hand. A common location for a GNSS antenna is the device itself, which provided −4 dB gain in [7]. The radiation patterns on the body are similar to what is measured here. Comparable efficiency was measured [10] where the antenna to body distance of 1 mm decreased the antenna gain to −19 dB.

The simulated performance of the BT antenna in close proximity to the hand decreased to −15 dB gain. The relative decrease in performance is almost similar in size to what was observed with the GNSS antenna. However, the difference between the antenna bent to the hand versus the antenna in straight position is 8 dB. Actually, the straight position is closer to the free space in performance than the antenna bent position. The BT antenna pattern in the phi0 cut changed from omnidirectional to directive with the maximum at 0 degrees. The antenna pattern in the phi90 cut changed away from the hand towards 0 degrees, but it also radiates ±90 and 180 degrees. Similar changes in radiation patterns

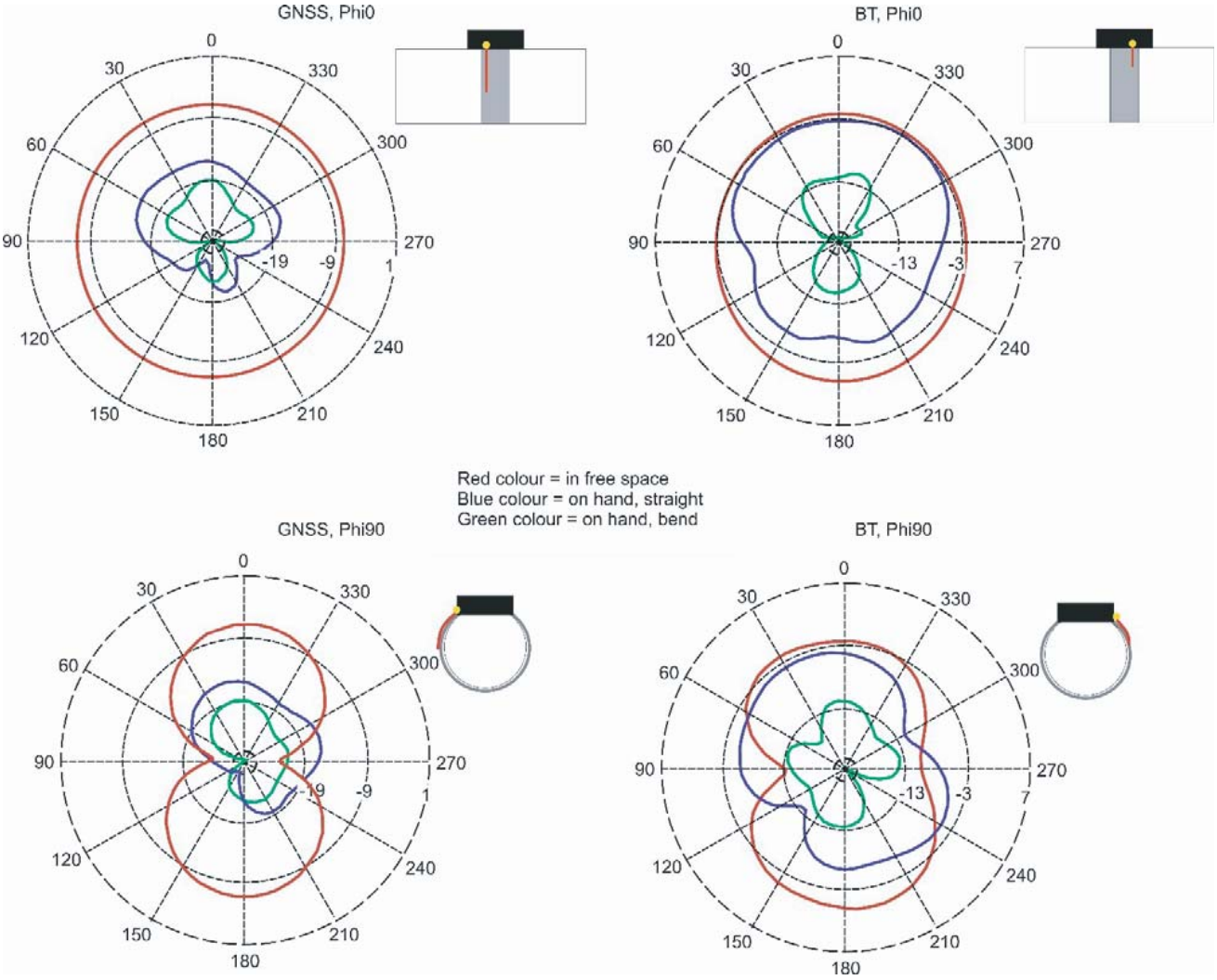

Figure 6. Simulated gain patterns of the GNSS and BT antennas in free space (red), on the hand in a straight position (blue), and on the hand in a bent position (green). Results on phi0 and phi90 cuts with SEBS material are presented.

were observed in [5] where the antenna was located on the wrist strip.

The measured antenna gain performances in free space are presented in Fig. 7. For the GNSS antenna, the simulated and measured results of the phi0 and phi90 cuts are close to each other. However, the BT antenna gain patterns are distorted compared to the earlier simulated ones. In the phi0 cut result, the TPU material antenna was closer to the simulated results, whereas the SEBS material antenna provided a flatter pattern directed towards ±90 degree angles. This is contrary to the phi90 cut, in which the pattern of SEBS material antenna was closer to simulated results, and the pattern of the TPU material antenna was more distorted than the simulated one. It was observed that the performance of the BT antenna decreased more than the GNSS antenna because it was more affected by the fabrication and material variance.

SAR values of the BT antenna were simulated with the standard hand models from CTIA and with 2.5 mW output power according to class 2 standard. The SAR distribution results are presented in Fig. 8. The maximum obtained SAR value was 0.55 W/kg, which is acceptable for the BT antenna. By comparing the obtained SAR result of the BT antenna, attention is paid to the small size (23 mm × 1 mm × 0.015 mm), the operating frequency of 2.45 GHz, and the antenna to body distance

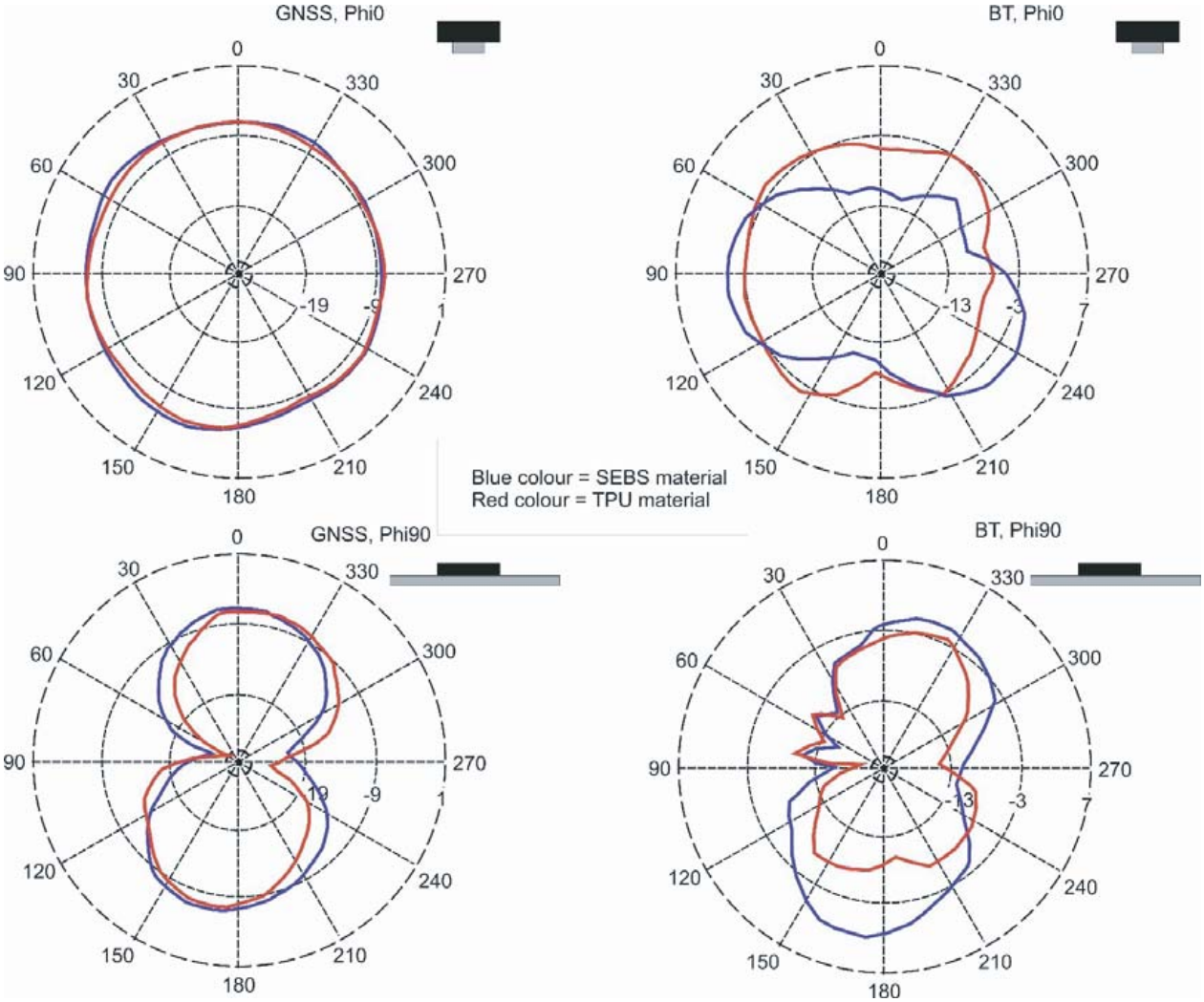

Figure 7. Measured E-field radiation patterns of the GNSS antenna on the phi0 and phi90 cuts with SEBS and TPU materials.

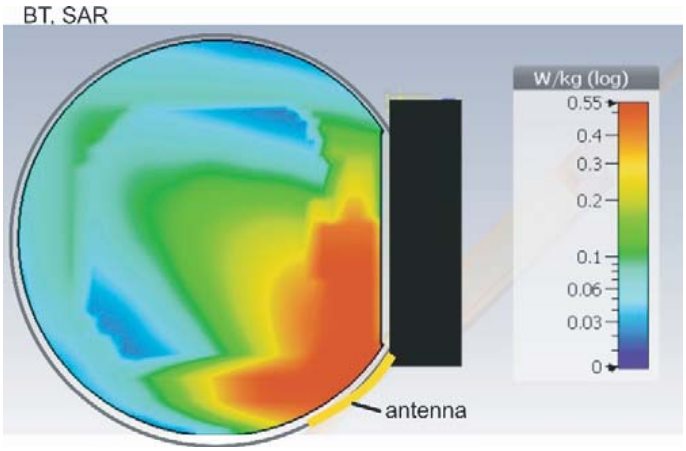

Figure 8. Simulated SAR distribution value of BT antenna with 2.5 mW power.

of 1 mm in contrast to [14], in which the ultra-wide band antenna size of 127 mm × 25 mm × 0.13 mm with a 2 mm antenna to the body distance was investigated. The ultra-wide band antenna exhibited increased SAR values of 3.75 W/kg at 850 MHz, 3.59 W/kg at 1900 MHz, and 3.45 W/kg at 2600 MHz for the wrist worn application.

4. CONCLUSION

In this paper, novel antennas implemented as F-shaped GNSS and L-shaped BT antennas for a wristwatch device and located on two sides of the wrist strap are presented, simulated, and measured. Two flexible low loss materials, TPU and SEBS (TC9), were investigated. Its integration on the flexible substrate material and covered with the PET material was proven to be feasible for a wearable smartwatch application. Experimental data suggest that the antenna can be used in the 1.575 GHz and 2.45 GHz bands.

The most relevant references for comparison are [4–8] where wristwatch devices were considered. Comparable antennas from a performance point of view are located on the wrist strip. It seems, however, that the wristwatch itself still provides a better location and performance for antennas than the wrist strip, where the efficiency was decreased. Some novel antenna structures [13–16] would be interesting to design on the wrist strip since their current performances were measured at a 5 mm distance from the body, whereas in this application the distance was only 0.8 mm.

New locations for the antennas and electronic modules were modelled and measured. Silver printing and molding technologies with new materials SEBS (TC9) were successfully utilized in wearable devices. The new materials SEBS (TC9) increased the total efficiency of the antennas by 1.6 dB for GNSS and by 2.2 dB for BT over the previously used materials (TPU).

New positions for antenna locations were studied for further improvement of devices; however, references show that previously used locations on the wristwatch device would still be better for these antenna structures. The PET material used for covering the antenna element on the substrate was observed to maintain antenna performance when the device was molded together.

Simulation versus measurement correlation was distorted due to the unfinished form of the current prototypes. For instance, the effect of contacts, variation of the antenna position in the base frame, cable assembly, pin, and its structure affected the final outcome. Further work is needed for antennas to optimize their electrical performance and minimize the manufacturing variances. The technique demonstrated good potential for realizing the mechanical structure of the product together with the printed antennas. Overmolded printed and hybrid integrated discrete antennas were proven feasible as an added-value flexible and seamless product structure but also low-cost mass manufacturing method. The research opens new perspectives for product definitions with a flexible, low loss material that would provide a better user experience in the market.

ACKNOWLEDGMENT

This work was funded and supported by Business Finland and the University of Oulu, co-innovation project Ruby (Connected quantitative sensing).

REFERENCES

1. Sankaralingam, S., S. Dhar, and B. Gupta, "Preliminary studies on performance of a 2.45 GHz wearable antenna in the vicinity of human body," *Proceedings of the 2012 International Conference on Communications, Devices and Intelligent Systems, CODIS 2012*, 2012.
2. Raad, H. K., H. M. Al-Rizzo, A. I. Abbosh, and A. I. Hammoodi, "A compact dual band polyimide based antenna for wearable and flexible telemedicine devices," *Progress In Electromagnetics Research C*, Vol. 63, 153–161, 2016.
3. Al-Sehemi, A., A. Al-Ghamdi, N. Dishovsky, G. Atanasova, and N. Atanasov, "A flexible planar antenna on multilayer rubber composite for wearable devices," *Progress In Electromagnetics Research C*, Vol. 75, 31–42, 2017.

4. Jia, Y., L. Liu, J. Hu, and L. J. Xu, "Miniaturized wearable watch antenna for wristband applications," *IEEE MTT-S 2019 International Microwave Biomedical Conference, IMBioC 2019 — Proceedings*, 2019.
5. Li, G., G. Gao, J. Bao, B. Yi, C. Song, and L. A. Bian, "A watch strap antenna for the applications of wearable systems," *IEEE Access*, Vol. 5, 2017.
6. Alkhamis, R., J. Wigle, and H. Song, "Global positioning system and distress signal frequency wrist wearable dual-band antenna," *Microw. Opt. Technol. Lett.*, 2057–2064, 2017.
7. Chen, J., M. Berg, V. Somero, H. Y. Amin, and A. Pärssinen, "A multiple antenna system design for wearable device using theory of characteristic mode," *European Conference on Antennas and Propagation*, London, UK, 2018.
8. Chung, M. A., "Embedded 3D multi-band antenna with ETS process technology covering LTE/WCDMA/ISM band operations in a smart wrist wearable wireless mobile communication device design," *IET Microwaves Antennas & Propagation*, Vol. 14, No. 12, 2020.
9. Ferreira, D., P. Pires, R. Rodrigues, and R. F. S. Caldeirinha, "Wearable textile antennas: Examining the effect of bending on their performance," *IEEE Antennas and Propagation Magazine*, Vol. 59, No. 3, 54–59, 2017.
10. Ismail, S., P. A. Gaydecki, and A. Barton, "A flexible wearable antenna for location tracking applications," *Int. J. Commun. Antenna. Propag.*, Vol. 8, No. 6, 494–499, 2018.
11. Prudhvi Nadh, B., B. T. P. Madhav, M. Siva Kumar, M. Venkateswara Rao, and T. Anilkumar, "Asymmetric ground structured circularly polarized antenna for ISM and WLAN band applications," *Progress In Electromagnetics Research M*, Vol. 76, 167–175, 2018.
12. Raad, H., "An UWB antenna array for flexible IoT wireless systems," *Progress In Electromagnetics Research*, Vol. 162, 109–121, 2018.
13. Bhattacharjee, S., S. Maity, S. R. B. Chaudhuri, and M. Mitra, "Compact dual-band dual-polarized omnidirectional antenna for on-body applications," *IEEE Transactions on Antennas and Propagation*, Vol. 67, No. 8, 5044–5053, 2019.
14. Bhattacharjee, S., M. Midya, M. Mitra, and S. R. B. Chaudhuri, "Dual band-dual polarized planar inverted F-antenna for MBAN applications," *International Journal of Microwave and Wireless Technologies*, Vol. 11, No. 1, 76–86, 2019.
15. Wang, W., X. W. Xuan, P. Pan, and Y. J. Hua, "A low-profile dual-band omnidirectional Alford antenna for wearable WBAN applications," *Microwave and Optical Technology Letters*, Vol. 62, No. 5, 2040–2046, 2020.
16. Bhattacharjee, S., S. Teja, M. Midya, S. R. B. Chaudhuri, and M. Mitra, "Dual band dual mode triangular textile antenna for body-centric communications," *URSI Asia-Pacific Radio Science Conference (AP-RASC)*, 1–4, 2019.
17. Flores-Cuadras, J. R., J. L. Medina-Monroy, R. A. Chavez-Perez, and H. Lobato-Morales, "Novel ultra-wideband flexible antenna for wearable wrist worn devices with 4G LTE communications," *Microw. Opt. Technol. Lett.*, Vol. 59, 777–783, 2017.